第 32 卷第 1 期
2016 年 1 月

无 机 化 学 学 报
CHINESE JOURNAL OF INORGANIC CHEMISTRY

Vol.32 No.1
167-174

基于 5-(3′,4′-二(四唑-5′-基)苯氧基)间苯二甲酸构筑的镧系金属配合物的合成、晶体结构及性质

陈小莉* 张潇戈 高楼军 马红燕

(延安大学化学与化工学院,陕西省反应工程重点实验室,延安 716000)

摘要: 在水热条件下利用 H_2btpa 配体合成了 2 个镧系金属配合物{[Ln(btpa)(H_2O)(OH)]·bpy}$_n$(Ln=Tb(**1**),Pr(**2**),H_2btpa=5-(3′,4′-二(四唑-5′-基)苯氧基)间苯二甲酸,bpy=4,4′-联吡啶),并用元素分析、红外光谱、X 射线粉末衍射、X 射线单晶衍射对其进行了表征。配合物 **1** 和 **2** 中,双核镧系金属单元通过 btpa^{2-}配体以 μ_4:η^1,η^2,η^1,η^2 的配位模式连接,形成二维网状结构,客体分子 4,4′-联吡啶通过分子间的氢键作用存在于结构中。相邻的二维网通过氢键的识别作用以锁链形式拓展为三维超分子结构。室温下配合物 **1** 呈现出 $Tb^{Ⅲ}$的特征荧光发射峰。

关键词: 镧系; 5-(3′,4′-二(四唑-5′-基)苯氧基)间苯二甲酸; 晶体结构; 荧光

中图分类号: O614.341; O614.33+4 **文献标识码**: A **文章编号**: 1001-4861(2016)01-0167-08

DOI: 10.11862/CJIC.2016.009

Syntheses, Crystal Structures and Properties of Two Lanthanide-Metal Complexes Based on Flexible 3′, 4′-Bis (terazol-5′-yl) phenoxy) isophthalic Acid

CHEN Xiao-Li* ZHANG Xiao-Ge GAO Lou-Jun MA Hong-Yan

(*School of Chemistry and Chemical Engineering, Shaanxi Key Laboratory of Chemical Reaction Engineering, Yan'an University, Yan'an, Shaanxi* 716000, *China*)

Abstract: Two novel lanthanide metal complexes based on H_2btpa ligand, namely {[Ln(btpa)(H_2O)(OH)]·bpy}$_n$ (Ln=Tb (**1**), Pr(**2**), H_2btpa=3′,4′-bis(terazol-5′-yl) phenoxy) isophthalic acid, bpy=4,4′-pyridine), have been synthesized and structurally characterized by elemental analyses, IR spectroscopy, powder X-ray diffraction and single-crystal X-ray diffraction analyses. They possess the same 2D network, which is constructed from binuclear lanthanide units cross-linked by btpa^{2-} ligands via μ_4:η^1,η^2,η^1,η^2 coordination mode with guest molecule bpy existing in the structure to form intermolecular hydrogen bond. Interestingly, the adjacent 2D networks are intercalated in a zipper fashion generating a 3D supramolecular structure through intermolecular hydrogen bonding. The luminescence experiments show that complex **1** exhibits typical $Tb^{Ⅲ}$-centered emissions in the visible region. CCDC: 1417525, **1**; 1417526, **2**.

Keywords: lanthanide; 3′,4′-bis(terazol-5′-yl)phenoxy)isophthalic acid; crystal structure; luminescence

Luminescent lanthanide metal-organic frameworks (MOFs) have attracted extensive attention, because of their fantastic topological structures and their technological importance, such as luminescence sensors, diagnostic tools, laser materials and optical amplification for telecommunications[1]. However,

收稿日期:2015-09-21。收修改稿日期:2015-10-30。

国家自然科学基金(No.21101133)和陕西省自然科学基础研究计划项目 (No.2014JM2056)资助。

*通信联系人。E-mail:chenxiaoli003@163.com;会员登记号:S06N7138M1005。

lanthanide ions are very poor at absorbing light directly, because of the low extinction coefficients of the Laporte forbidden *f-f* transitions[2]. Energy transfer from an adjacent strongly absorbing chromophore is usually used to stimulate luminescence from lanthanides. In this regard, the ligands with good light absorptivity and strong coordination capability to lanthanide ions should be selected as building units for lanthanide-organic hybrid. Polycarboxylic acids have been selected as building units, given that lanthanide ions have a high affinity for hard donor atoms. Carboxylate group not only acts as efficient sensitizers for lanthanide emission but also as the functional group can coordinate to metal ions in several different binding modes. Therefore, lanthanide polycarboxylic complexes have good luminescent properties and fascinating structures. Especially, polycarboxylate ligands are usually employed in the architectures for lanthanide coordination polymers [3]. However, the majority of these reports have focused on the complexes with rigid carboxylate ligands. The use of flexible ligands as building blocks in the construction of coordination frameworks is attractive because the flexibility and conformational freedoms of the ligands may offer various possibilities for construction of frameworks with unique structures and useful properties[4]. But lanthanide complexes based on flexibility carboxylate ligands have been rarely used in this aspect[5].

As a member of flexible carboxylic acids ligands, 3′,4′-bis(terazol-5′-yl) phenoxy) isophthalic acid (H_2btpa) contains multi-oxygen and nitrogen atoms and can coordinate with metal ions in different ways, resulting in the formations of various MOFs with specific topologies and useful properties. Furthermore, they can act not only as hydrogen bond donors but also acceptors, which make them a wonderful candidate for the construction of supramolecular networks depending upon the number of deprotonated carboxylate groups. Therefore, H_2btpa may be an excellent candidate for the construction of multidimensional coordination polymers. However, to the best of our knowledge, btpa-metal complex have never been reported. We also notice that the introduction of N-containing auxiliary ligands such as 4,4′-bipyridine (bpy), 1,2-bis (4-pyridyl)ethylene (bpee), 1,2-bis (4-pyridyl) ethane (bpe) or 1,10-phenanthroline (phen) via adjustment of the carboxylate bridging mode into the system may lead to new structural evolution and fine-tuning the structural motif of the complexes[6]. The design and elaborate assembly of multidimensional lanthanide-based MOFs with these kind of flexible ligands are still challenging tasks because of high and variable coordination numbers of lanthanide ions and versatile conformation of the ligands. With the aim of understanding the coordination chemistry of them and studying the influence on the framework structure of the complexes, we have recently engaged in the research of this kind of complex. Fortunately, we have obtained two new lanthanide complexes, $\{[Ln(btpa)(H_2O)(OH)]\cdot bpy\}_n$ (Ln = Tb (**1**), Pr (**2**)). Herein we described the syntheses, structures, the thermal stabilities and luminescent properties of these complexes.

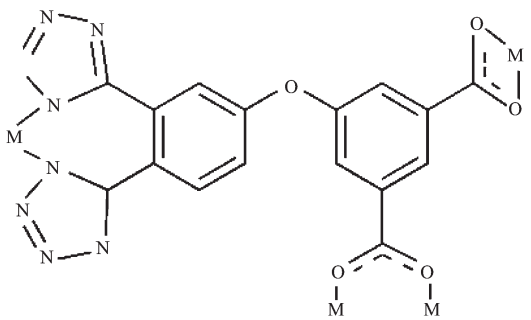

Scheme 1 Coordination mode of H_2btpa in **1** and **2**

1 Experimental

1.1 Reagents and physical measurements

All chemicals and reagents were used as received from commercial sources without further purification. All reactions were carried out under hydrothermal conditions. Elemental analyses (C, H, N) were determined with a Elementar Vario EL Ⅲ elemental analyzer. IR spectra were recorded as KBr pellets on a Bruker EQUINOX55 spectrophotometer in the 4 000 ~400 cm^{-1} region. Fluorescence spectra were performed on a Hitachi F-4500 fluorescence spectrophotometer at room temperature. Thermogravimetric analyses (TGA) were performed in a nitrogen

atmosphere with a heating rate of 10 ℃·min^{-1} with a NETZSCHSTA 449C thermogravimetric analyzer. The X-ray powder diffraction pattern was recorded with a Rigaku D/Max 3 Ⅲ diffractometer operating at 40 kV and 30 mA using Mo $K\alpha$ radiation (λ=0.154 18 nm).

1.2 Synthesis of {[Tb(btpa)(H_2O)(OH)]·bpy}$_n$ (1)

A mixture of $Tb(NO_3)_3·5H_2O$ (0.2 mmol, 0.087 g), H_2btpa (0.1 mmol, 0.039 4 g), bpy (0.1 mmol, 0.018 2 g) and NaOH (0.4 mmol, 0.016 g) in water (10 mL) was stirred for 30 min in air, then sealed in a 15 mL Telfon-lined stainless steel container, which was heated to 160 ℃ for 96 h. After cooling to room temperature at a rate of 5 ℃·h^{-1}, colorless crystals were obtained in *ca.* 42% yield based on Tb. Anal. Calcd. for $C_{26}H_{15}N_{10}O_7Tb$ (%): C, 42.29; H, 2.05; N 18.97. Found (%): C, 42.24; H, 2.08; N, 18.99. FTIR (KBr, cm^{-1}): 3 442(s), 3 074(w), 1 619(s), 1 576(s), 1 454(s), 1 389(s), 1 276(m), 1 210(m), 1 103(w), 979 (m), 783(m), 614(w).

1.3 Synthesis of {[Pr(btpa)(H_2O)(OH)]·bpy}$_n$ (2)

The colorless crystals of **2** were prepared by a similar method used in the synthesis of crystals of **1** except that $Tb(NO_3)_3·5H_2O$ was replaced by $Pr(NO_3)_3·5H_2O$ (49 % yield based on Pr). Anal. Calcd for $C_{26}H_{15}N_{10}PrO_7$(%): C, 43.35; H , 2.10; N, 19.45. Found (%): C, 43.27; H, 2.25; N, 19.43 %. FTIR (KBr, cm^{-1}): 3 437(s), 3 074(w), 2 921(w), 1 619(s), 1 579(s), 1 445(s), 1 386(s), 1 240(m), 1 209(m), 1 103(w), 979 (m), 783(m), 617(w).

1.4 X-ray crystallography

Intensity data were collected on a Bruker Smart APEX II CCD diffractometer with graphite-monochromated Mo $K\alpha$ radiation (λ=0.071 073 nm) at room temperature. Empirical absorption corrections were applied using the SADABS program [7a]. The structures were solved by direct methods and refined by the full-matrix least-squares based on F^2 using SHELXTL-97 program [7b]. All non-hydrogen atoms were refined anisotropically and hydrogen atoms of organic ligands were generated geometrically. Crystal data and structural refinement parameters for **1** and **2** are summarized in Table1, and selected bond distances and bond angles are listed in Table 2.

CCDC: 1417525, **1**; 1417526, **2**.

Table 1 Crystal data and structural refinement parameters for the title complexes 1 and 2

Complex	**1**	**2**
Empirical formula	$C_{26}H_{15}N_{10}O_7Tb$	$C_{26}H_{15}N_{10}O_7Pr$
Formula weight	738.40	720.40
Crystal system	Monoclinic	Monoclinic
Space group	*C*2/*m*	*C*2/*m*
a / nm	1.462 69(11)	1.483 3(8)
b / nm	1.624 72(11)	1.632 1(8)
c / nm	1.104 92(8)	1.118 8(6)
β / (°)	97.917(10)	97.783(10)
V / nm^3	2.600 8(3)	2.683 6(2)
Z	4	4
D_c / (g·cm^{-3})	1.886	1.786
F(000)	1 448	1 428
Crystal size / mm	0.33×0.30×0.28	0.34×0.32×0.30
Absorption coefficient / mm^{-1}	2.789	1.883
Reflections collected	6 728	6 908
R_{int}	0.026 1	0.023 5
Limiting indices	$-17\leqslant h\leqslant 17$, $-10\leqslant k\leqslant 19$, $-13\leqslant l\leqslant 13$	$-17\leqslant h\leqslant 17$, $-19\leqslant k\leqslant 12$, $-12\leqslant l\leqslant 13$
Goodness-of-fit on F^2	1.079	1.064
R_1, wR_2 ($I>2\sigma(I)$)	0.027 5, 0.070 4	0.021 4, 0.054 6
R_1, wR_2 (all data)	0.026 6, 0.069 7	0.023 6, 0.055 8

Table 2 Selected bond distances(nm) and bond angles(°) for complexes 1 and 2

Complex **1**					
Tb(1)-O(1A)	0.225 5(3)	Tb(1)-O(2B)	0.228 9(3)	Tb(1)-O(6)	0.237 0(4)
Tb(1)-O(6A)	0.237 0(4)	Tb(1)-O(3A)	0.250 0(8)	Tb(1)-O(4A)	0.239 3(7)
Tb(1)-N(1)	0.256 9(3)	Tb(1)-N(1D)	0.256 9(3)		
O(1)-Tb(1)-O(2)	92.56(12)	O(1)-Tb(1)-O(6)	88.82(12)	O(2)-Tb(1)-O(6)	74.29(8)
O(6)-Tb(1)-O(6)	148.35(18)	O(1)-Tb(1)-O(4)	143.8(2)	O(2)-Tb(1)-O(4)	123.7(2)
O(2)-Tb(1)-O(4)	100.21(13)	O(1)-Tb(1)-O(4A)	143.0(2)	O(2)-Tb(1)-O(4A)	118.9(2)
O(6)-Tb(1)-O(4A)	82.3(2)	O(4)-Tb(1)-O(4A)	17.89 (18)	O(4A)-Tb(1)-O(4A)	35.2(4)
O(1)-Tb(1)-O(3)	160.4(2)	O(2)-Tb(1)-O(3)	76.2(2)	O(6)-Tb(1)-O(3)	72.8(2)
O(6)-Tb(1)-O(3)	103.2(2)	O(4)-Tb(1)-O(3)	49.9(3)	O(4A)-Tb(1)-O(3)	55.4(3)
O(4A)-Tb(1)-O(3)	42.9(3)	O(1)-Tb(1)-O(3)	160.4(2)	O(3)-Tb(1)-O(3)	31.6(4)
O(1)-Tb(1)-O(3A)	164.9(2)	O(2)-Tb(1)-O(3A)	72.3(2)	O(6)-Tb(1)-O(3A)	87.07(11)
O(3A)-Tb(1)-N(1)	113.78(17)	O(4)-Tb(1)-N(1)	71.63(19)	O(4)-Tb(1)-O(3A)	51.3(3)
O(4A)-Tb(1)-O(3A)	50.5(3)	O(3)-Tb(1)-O(3A)	16.1(2)	O(1)-Tb(1)-N(1)	78.47(10)
O(2)-Tb(1)-N(1)	144.54(8)	O(6)-Tb(1)-N(1)	138.64(11)	O(6)-Tb(1)-N(1)	71.32(11)
O(4)-Tb(1)-N(1)	71.6(2)	O(4A)-Tb(1)-N(1)	64.7(2)	O(4A)-Tb(1)-N(1)	84.78(19)
O(3)-Tb(1)-N(1)	119.9(2)	O(3)-Tb(1)-N(1)	101.3(2)	N(1)-Tb(1)-N(1)	67.63(15)
Complex **2**					
Pr(1)-O(1)	0.234 0(2)	Pr(1)-O(4A)	0.246 7(7)	Pr(1)-O(2A)	0.236 9(3)
Pr(1)-O(6)	0.246 8(6)	Pr(1)-O(3A)	0.256 5(7)	Pr(1)-O(4)	0.245 4(6)
Pr(1)-N(4E)	0.265 5(2)	Pr(1)-N(4D)	0.265 5(2)	Pr(1)-O(3)	0.255 2(6)
O(1)-Pr1-O(2)	92.97(9)	O(4)-Pr(1)-O(3)	50.79(19)	O(1)-Pr(1)-O(4)	142.59(16)
O(6)-Pr(1)-O(3)	86.97(8)	O(1)-Pr(1)-O(6)	89.47(8)	O(4A)-Pr(1)-O(3)	50.4(2)
O(2)-Pr(1)-O(4)	124.44(16)	O(1)-Pr(1)-O(3A)	161.99(18)	O(2)-Pr(1)-O(6)	74.55(6)
O(2)-Pr(1)-O(3A)	76.82(17)	O(4)-Pr(1)-O(6)	99.77(9)	O(4)-Pr(1)-O(3A)	49.7(2)
O(6)-Pr(1)-O(6)	148.98(13)	O(6A)-Pr(1)-O(3A)	73.61(19)	O(1)-Pr(1)-O(4A)	141.81(16)
O(6)-Pr(1)-O(3A)	101.77(18)	O(2)-Pr(1)-O(4A)	120.61(16)	O(4A)-Pr(1)-O(3A)	44.0(2)
O(4)-Pr(1)-O(4A)	16.49(15)	O(4A)-Pr(1)-O(3A)	54.72(2)	O(6)-Pr(1)-O(4A)	83.31(17)
O(3)-Pr(1)-O(3A)	14.86(17)	O(6)-Pr(1)-O(4A)	115.16(18)	O(3A)-Pr(1)-O(3A)	29.2(3)
O(4A)-Pr(1)-O(4A)	32.6(3)	O(1)-Pr(1)-N(4)	77.93(8)	O(1)-Pr(1)-O(3)	166.62(15)
O(2)-Pr(1)-N(4)	145.09(5)	O(2)-Pr(1)-O(3)	73.65(15)	O(4)-Pr(1)-N(4)	70.96(13)
O(6)-Pr(1)-N(4)	137.91(8)	O(6)-Pr(1)-N(4)	137.91(8)	N(4)-Pr(1)-N(4)	66.37(11)
O(4A) -Pr(1)-N(4)	82.65(16)	O(3A) -Pr(1)-N(4)	118.81(17)	O(3)-Pr(1)-N(4)	113.02(12)

Symmetry codes: A: $-x$, y, $-z$; B: $x+1/2$, $y+1/2$, z; D: $-x$, $-y$, $-z$; E: x, $-y$, z for **1**; A: $-x$, y, $-z$; D: $-x+1/2$, $y+1/2$, $-z$; E: $-x$, $-y$, $-z$ for **2**

2 Results and discussion

2.1 Structure description of complexes 1 and 2

Complexes **1** and **2** are isomorphism and exhibit the same network structure, so only **1** is depicted in detail. Single-crystal X-ray diffraction analysis reveals that complex **1** is a 2D network structure crystallized in monoclinic system with *C*2/*m* space group. The asymmetric unit of **1** contains one independent Tb^{III} ion, one $btpa^{2-}$ ligand, one coordinated water molecule, one coordinated hydroxyl group and one guest bpy molecule. As shown in Fig.1a, each Tb1 center is coordinated by two nitrogen atoms (Tb1-N1 0.256 9(3) nm, Tb1-N1D 0.256 9(3) nm) from one $btpa^{2-}$ ligand, four oxygen atoms (O1A, O2B, O3A and O4A) from three bridging $btpa^{2-}$ ligands, one oxygen atom from a

coordinated water molecule and one hydroxyl group oxygen atom. The coordination geometry of Tb1 atom can be best described as distorted dodecahedron geometry (Fig.1b). The Tb1-O bond lengths are in the range of 0.228 9(3)~0.249 9(9) nm. The O-Tb1-O bond angles vary from 16.1(2)° to 164.9(2)°. All of them are similar to those found in the related terbium-oxygen donor compounds[8].

It is noteworthy that completely deprotonated $btpa^{2-}$ ligand adopts a μ_4:η^1,η^2,η^1,η^2 coordination mode. One carboxylate group coordinates with two Tb^{III} ions bimonodentately; the other carboxylate group coordinates with one Tb^{III} ion in bidentate-chelating way; two terazo nitrogen atoms chelate with one Tb^{III} ion (Scheme 1). Each $btpa^{2-}$ ligand bridges four Tb^{III} ions. The $btpa^{2-}$ anion is largely bent at the ether bond site (∠O-C-O 124.67(6)° for **1**, 124.33(6)° for **2**). The dihedral angle between the two phenyl rings is 79.93° for **1**, and 79.94(6)° for **2**.

On the basis of the connection mode, each pair of Tb^{III} centers are bridged by two carboxylate groups from two $btpa^{2-}$ ligands to form a cyclic binuclear unit with the Tb1 ⋯ Tb1 distances of 0.533 3 nm. The neighboring Tb1 dimeric units are linked by four carboxylate groups of four $btpa^{2-}$ ligands generating a 1D ring chain with the intrachain Tb1⋯Tb1 distances of 1.104 9 nm. The adjacent 1D ring chains are parallel to each other, in which Tb1 dimeric unit further linked by (μ_3:η^1,η^1,η^2) $btpa^{2-}$ ligands to form infinite 2D network structure along the *a* axis (Fig.2).

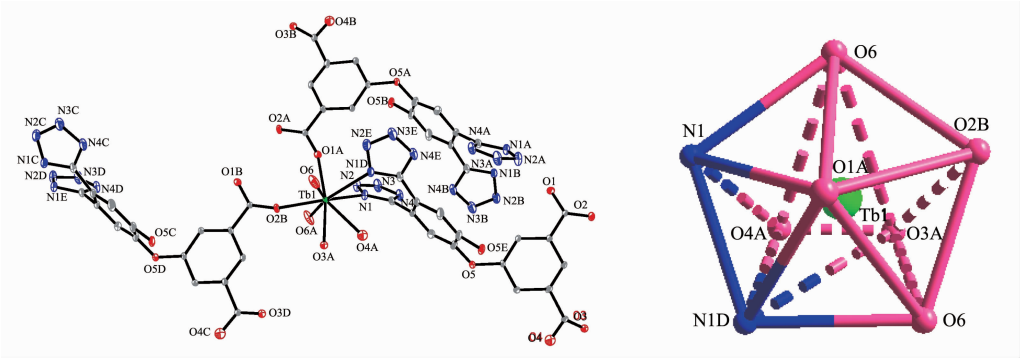

Ellipsoid probability was drawn at 30%; all H atoms are omitted for clarity; Symmetry code: A: −*x*, *y*, −*z*; B: *x*+1/2, *y*+1/2, *z*; C: −*x*+1/2, *y*+1/2, −*z*; D: −*x*, −*y*, −*z*; E: *x*, −*y*, *z*

Fig.1　(a) Coordination environment of the Tb^{III} ion in **1**; (b) View of dodecahedron geometry of Tb^{III} ion

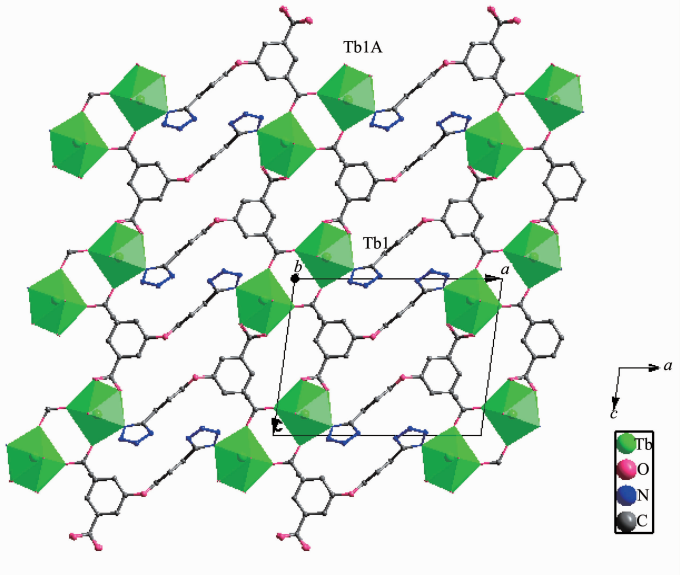

Symmetry code: A: −*x*, *y*, −*z*

Fig.2　View of the 2D network structure based on μ_4-bridging $btpa^{2-}$ ligand along b-axis

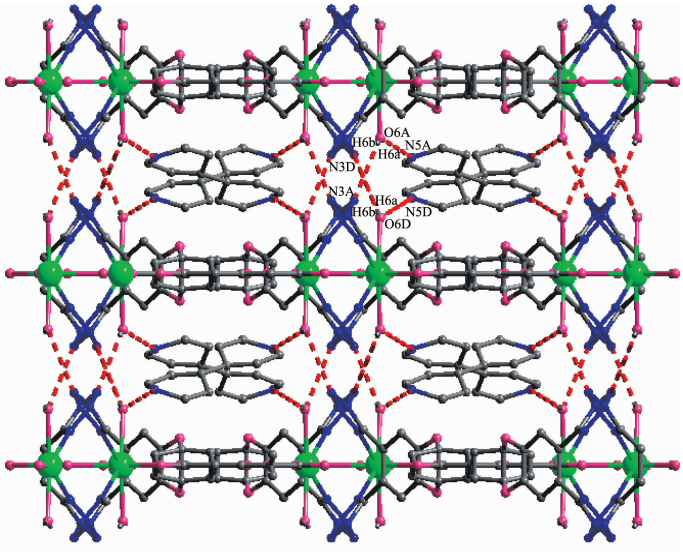

Symmetry codes: A: $-x$, y, $-z$; D: $-x$, $-y$, $-z$

Fig.3 View of the 3D supramolecular architecture based on hydrogen bonding interaction along *a*-axis

It is also noteworthy that the 2D framework forms a novel $\{Tb_2N_2O_4C_{18}\}$ 26-membered ring containing a type of rhombic pore with size of *ca.* 1.148 5 nm × 0.915 6 nm based on the distances of Tb1…Tb1A and O5 … O5. Interestingly, the adjacent 2D network recognize each other in a zipper fashion to generate a 3D supramolecular framework through hydrogen bonding interaction between the guest bpy molecules and coordinated water molecules (O6A-H6a … N5A 0.271 9 nm, 167.47°; Symmetry codes: A: $-x$, y, $-z$). Moreover, significant hydrogen bond interaction (O6A-H6b … N3A 0.305 3 nm, 145.54°) contributes to the additional stability of the structure (Fig.3).

2.2 IR spectra of 1 and 2

The IR spectra of **1** and **2** are fully identical. In the FTIR spectra, the absorption bands in the region 3 430~3 442 cm^{-1} may attribute to the stretching vibrations of O-H and N-H. The bands in the region 2 920~3 074 cm^{-1} can be ascribed to C-H stretching vibrations of the benzene ring [9]. The absence of the absorption bands at 1 730~1 690 cm^{-1} in **1** and **2** indicates the H_2btpa ligand adopts the complete deprotonated $btpa^{2-}$ form, which is consistent with the X-ray structural analysis. The asymmetric stretching vibrations of the carboxylate groups are observed at 1 619 and 1 576 cm^{-1}, and the symmetric stretching vibration (ms) of the carboxylate groups is observed at 1 454 and 1 389 cm^{-1}, respectively[3a]. The separation $\Delta\nu$(COO) between the ν_{as}(COO) and ν_s(COO) band in **1** is 165 and 187 cm^{-1}, which is smaller than 200 cm^{-1}, indicating that the carboxyl groups are coordinated in bridging mode [10]. The bands in the region of 1 210 cm^{-1} and 1 209 cm^{-1} for **1** and **2** can be assigned to the C-O-C stretching vibrations.

2.3 Luminescent properties

The photoluminescence properties of complexes **1** and **2** were examined at room temperature, and the emission spectra are shown in Fig.4. The ligand-centered luminescence is completely disappeared in complex **1**, whereas the typical narrow emission bands of Tb^{III} ions can be detected upon excitation of the ligand-centered absorption bands (Fig.4a). For **1**, the emission spectrum excited upon 350 nm shows the characteristic emission bands at 490, 545, 586 and 620 nm attributed to $^5D_4 \rightarrow {}^7F_J$ (J=6, 5, 4, and 3) transitions [11], indicating that $btpa^{2-}$ ligand is good sensitizer for Tb^{III} luminescence. The $^5D_4 \rightarrow {}^7F_5$ transition is the strongest among the four bands, showing higher color purity and emission intensity. The luminescence of **2** and free ligand were also investigated, shown in Fig.4b. The ligand exhibits one emission band at 389 nm upon excitation at 315 nm. Complex **2** exhibits two intense emission peaks at ca. 420 and 438 nm at the same excitation condition,

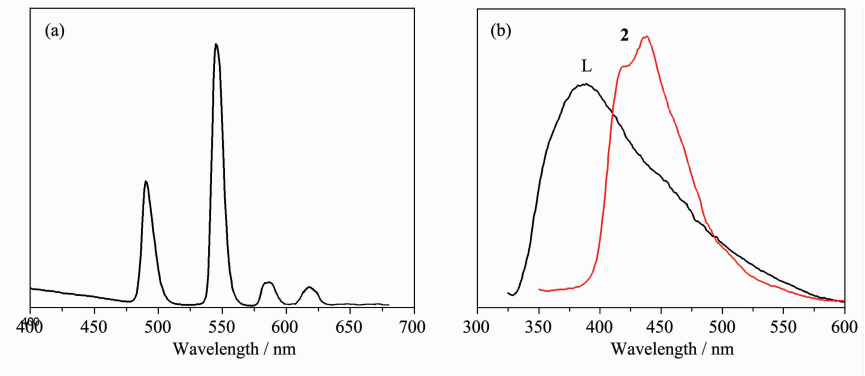

Fig.4　Emission spectra of **1**(a), **2** and ligand (b) in the solid state at room temperature

which means a red shift relative to that of the free ligand (λ_{max}=389 nm). It may be tentatively assigned to ligand to metal charge transfer (LMCT) [12]. By comparing the emission spectra of **2** and ligand, we can conclude that the enhancement of luminescence in **1** and **2** may be attributed to the ligation of ligand to the metal center, which effectively increases the rigidity and reduces the loss of energy by radiationless decay[13].

2.4　Thermal properties and PXRD measurement of complexes 1 and 2

To study the thermal stabilities of these complexes, thermal gravimetric analysis (TGA) were performed. The TG curves of **1** and **2** are shown in Fig.5. The isostructural frameworks lead to the similar thermal decomposition processes, so we took **1** as a representative example for thermogravimetric analysis. Complex **1** first lost its coordinated water molecules and hydroxyl group below 165 ℃, the weight loss of 4.78% was consistent with that calculated (4.74%). The second weight loss is 21.1% in the temperature range of 165~350 ℃ corresponding to the removal of

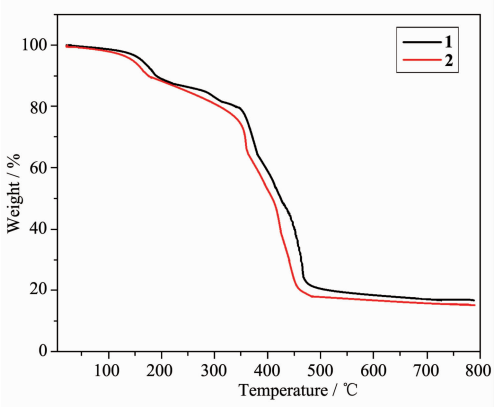

Fig.5　TGA curves of complexes **1** and **2**

guest bpy molecules (Calcd. 21.7%). The weight loss of 52.9% in the range of 350~485 ℃ was assigned to the decomposition $btpa^{2-}$ ligands (Calcd. 52.4%).

In order to confirm the phase purity of the bulk materials, powder X-ray diffraction (PXRD) patterns were measured at room temperature. The PXRD experimental and computer-simulated patterns of all of them are shown in Fig.6. The peaks of the simulated and experimental PXRD patterns are in good agreement with each other, confirming the phase purities of **1** and **2**.

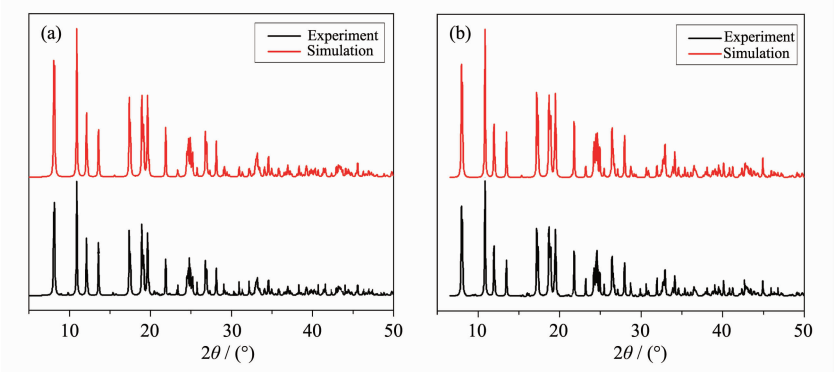

Fig.6　PXRD patterns of complexes **1** (a) and **2** (b)

3 Conclusions

In summary, two novel lanthanide complexes based on flexible H_2btpa ligand have been successfully synthesized and characterized. The crystal structures of $\{[Ln(btpa)(H_2O)(OH)]bpy\}_n$ (Ln=Tb (**1**), Pr (**2**)) reveal a distorted dodecahedron geometry around the Ln^{III} ions. Complexes **1** and **2** show the same 2D network structure, which is constructed from binuclear lanthanide units cross-linked by $btpa^{2-}$ ligands via μ_4: $\eta^1,\eta^2,\eta^1,\eta^2$ coordination mode with guest molecule bpy existing in the structure to form intermolecular hydrogen bond. The studies of luminescence properties show that complex **1** exhibited typical intense luminescence in the visible region.

References:

[1] (a) Rocha J, Carlos L D, Paz F A A, et al. *Chem. Soc. Rev.*, **2011**,**40**:926-940
(b) Carlos L D, Ferreira R A S, Bermudez V Z, et al. *Chem. Soc. Rev.*, **2011**,**40**:536-549
(c) Gai Y L, Jiang F L, Hong M C, et al. *Inorg. Chem.*, **2013**, **52**:7658-7665
(d) Cui Y, Yue Y, Chen B, et al. *Chem. Rev.*, **2012**,**112**: 1126-1162

[2] Bünzli J-C G, Choppin G R. *Lanthanide Probes in Life, Chemical and Earth Sciences*: *Theory and Practice*. Amsterdam: Elsevier, **1989**.

[3] (a) Xia J, Wang H S, Shi W, et al. *Inorg. Chem.*, **2007**,**46**: 3450-3458
(b) Zhang J, Zheng B, Zhao T T, et al. *Cryst. Growth Des.*, **2014**,**14**:2394-2400
(c) Gai Y L, Jiang F L, Hong M C, et al. *Cryst. Growth Des.*, **2014**,**14**:1010-1017
(d) Daiguebonne C, Kerbellec N, Bernot K, et al. *Inorg. Chem.*, **2006**,**45**:5399-5406
(e) Kerbellec N, Kustaryono D, Haquin V, et al. *Inorg. Chem.*, **2009**,**48**:2837-2843
(f) Huang W, Wu D Y, Meng Q J, et al. *Cryst. Growth Des.*, **2009**,**9**:1361-1369
(g) Reineke T M, Eddaoudi M, Yaghi O M, et al. *J. Am. Chem. Soc.*, **2000**,**122**:4843-4844

[4] (a) Zhu H F, Zhang Z H, Okamura T, et al. *Cryst. Growth Des.*, **2005**,**5**:177-182
(b) Kim Y J, Suh M, Jung D Y. *Inorg. Chem.*, **2004**,**43**:245-250

[5] (a) Yang J, Song S Y, Ma J F, et al. *Cryst. Growth Des.*, **2011**, **11**:5469-5474
(b) Liu G F, Qiao Z P, Chen X M, et al. *New J. Chem.*, **2002**,**26**:791-795
(c) Shi W J, Hou L, Zhao W, et al. *Inorg. Chem. Commun.*, **2011**,**14**:1915-1919
(d) Xiao D R, Li Y G, Wang E B, et al. *Inorg. Chem.*, **2007**, **46**:4158-4166
(e) Hou G F, Li H X, Li W Z, et al. *Cryst. Growth Des.*, **2013**,**13**:3374-3380

[6] (a) Lightfoot P, Snedden A. *J. Chem. Soc. Dalton Trans.*, **1999**:3549-3551
(b) Lee S W, Kim H J, Lee Y K, et al. *Inorg. Chim. Acta*, **2003**,**353**:151-158
(c) Sun C Y, Li L C, Jin L P. *Polyhedron*, **2006**,**25**:3017-3024
(d) Ahmad M, Sharma M K, Das R, et al. *Cryst. Growth Des.*, **2012**,**12**:1571-1578

[7] (a) Sheldrick G M. *SADABS*, University of Göttingen, Germany, **1996**.
(b) Sheldrick G M. *SHELXS*-97 *and SHELXL*-97, *Program for X-ray Crystal Structure Solution and Refinement*, University of Göttingen, Germany, **1997**.

[8] Li X, Wu X S, Zheng X J. *Inorg. Chim. Acta*, **2009**,**362**: 2537-2541

[9] Chen S, Fan R Q, Sun C F, et al. *Cryst. Growth Des.*, **2012**,**12**:1337-1346

[10] Nakamoto K, Translated by HUANG De-Ru (黄德如), WANG Ren-Qing (汪仁庆), WEI Xin-Cheng (卫新成). *Infrared Raman Spectra of Inorganic and Coordination Compounds* (无机和配位化合物的红外和拉曼光谱). Beijing: Chemical Industry Press, **1986**:235

[11] Katkova M A, Borisov A V, Fukin G K, et al. *Inorg. Chim. Acta*, **2006**,**359**:4289-4296

[12] (a) Ganesan S V, Natarajan S. *Inorg. Chem.*, **2004**,**43**:198-205
(b) Valeur B. *Molecular Fluorescence*: *Principles and Applications*. Weinheim: Wiley-VCH, **2002**.

[13] (a) Zhang L Y, Liu G F, Zheng S L, et al. *Eur. J. Inorg. Chem.*, **2003**:2965-2971
(b) Wang X L, Qin C, Wang E B, et al. *Angew. Chem., Int. Ed.*, **2004**,**43**:5036-5040